Charge Translocation by the Na^+/K^+-ATPase Investigated on Solid Supported Membranes: Rapid Solution Exchange with a New Technique

J. Pintschovius and K. Fendler
Max-Planck-Institut für Biophysik, D-60596 Frankfurt/Main, Germany

ABSTRACT Adsorption of Na^+/K^+-ATPase containing membrane fragments from pig kidney to lipid membranes allows the detection of electrogenic events during the Na^+/K^+-ATPase reaction cycle with high sensitivity and time resolution. High stability preparations can be obtained using solid supported membranes (SSM) as carrier electrodes for the membrane fragments. The SSMs are prepared using an alkanethiol monolayer covalently linked to a gold surface on a glass substrate. The hydrophobic surface is covered with a lipid monolayer (SAM, self-assembled monolayer) to obtain a double layer system having electrical properties similar to those of unsupported bilayer membranes (BLM). As we have previously shown (Seifert et al., 1993, *Biophys. J.* 64:384–391), the Na^+/K^+-ATPase on a SSM can be activated by photolytic release of ATP from caged ATP. In this publication we show the first results of a new technique which allows rapid solution exchange at the membrane surface making use of the high mechanical stability of SSM preparations. Especially for substrates, which are not available as a caged substance—such as Na^+ and K^+—this technique is shown to be capable of yielding new results. The Na^+/K^+-ATPase was activated by rapid concentration jumps of ATP and Na^+ (in the presence of ATP). A time resolution of up to 10 ms was obtained in these experiments. The aim of this paper is to present the new technique together with the first results obtained from the investigation of the Na^+/K^+-ATPase. A comparison with data taken from the literature shows considerable agreement with our experiments.

INTRODUCTION

Electrical measurements of ion translocating membrane protein experiments can be divided into two classes: steady-state and pre-steady-state experiments. Steady-state experiments are carried out to establish whether the transport as a whole is electrogenic, electrogenicity of transport being of physiological importance. The steady-state electrical activity at different applied voltages can be used to gain information about the transport cycle of the enzyme (Schwarz and Vasilets, 1991; Gadsby and Nakao, 1989). However, the relationship of overall electrogenicity with the transport mechanism of the membrane protein is not straightforward. In pre-steady-state electrical measurements, the additional dimension introduced by the time dependence of the charge movement can yield more detailed information. Under favorable circumstances the charge translocation can be assigned to a specific step in the reaction cycle (Borlinghaus et al., 1987; Fendler et al., 1987, 1993).

In a pre-steady-state experiment, the steady state is perturbed by a rapid change of one of the parameters influencing the enzyme activity, so that its relaxation into the new steady state can be monitored. Conventionally, the perturbation consists of a rapid change of substrate concentration, of temperature, or of the applied voltage. However, the methods of perturbation are not always compatible with the experimental requirements. Direct electrical measurements require two electrically separated compartments, which are accessible to the electrodes. The barrier between the compartments usually is a fragile lipid membrane (BLM, black lipid membrane) representing a considerable problem if combined, e.g., with rapid mixing methods.

One approach to overcome this problem was the application of the patch-clamp technique using small-tipped pipettes. The membranes of the cells, having a diameter of ~ 1 μm, are sufficiently stable to sustain a rapid solution exchange (Franke et al., 1987). In order to obtain detectable signal currents, the application of patches with such small surface areas is restricted to ion channels, which usually have transport rates 1,000–10,000 times higher than membrane proteins carrying out active transport, such as ion translocating ATPases.

The problem of combining large area membranes for the investigation of ion translocating ATPases with concentration jump techniques was partly solved by the introduction of photolytically releasable substrates (Kaplan et al., 1978; McCray and Trentham, 1980), the so-called caged substrates. A number of membrane proteins were investigated either on artificial lipid bilayers (for a review see Bamberg et al., 1993) or on giant patches of cell membranes (Friedrich et al., 1996). However, only a few substrates are available as a caged substance. Also, a caged substrate can act as a competitive inhibitor (Fendler et al., 1993) or the cage itself may present a problem (McCray et al., 1980; Seifert et al., 1993).

For the reasons detailed above, we have made an attempt to exploit the high mechanical stability of solid supported membranes (SSM, Seifert et al., 1993) in combination with a rapid mixing technique. Concentration jumps of ATP and Na^+ could be generated to activate the Na^+/K^+-ATPase. A

Received for publication 24 February 1998 and in final form 18 September 1998.

Address reprint requests to Dr. Klaus Fendler, Max-Planck-Institut für Biophysik, Kennedyallee 70, D-60596 Frankfurt/M, Germany. Tel.: 49-69-6303-306; Fax: 49-69-6303-305; E-mail: fendler@biophys.mpg.de.

0006-3495/99/02/814/13 $2.00

time resolution up to 10 ms was obtained. The data generated by the rapid injection of ATP (in the presence of Na^+) and Na^+ (in the presence of ATP) at the solid supported membrane are compared to the results of previous concentration jump experiments performed with caged ATP (Borlinghaus et al., 1987; Fendler et al., 1985; 1987, 1993; Nagel et al., 1987). The two approaches are shown to yield consistent results. The possibility of electrical signal currents being a result of artefacts caused by the rapid stirring conditions of the experimental method is ruled out.

MATERIALS AND METHODS

Chemicals

Standard solutions contained 25 mM imidazole, 3 mM $MgCl_2$, 0.2 mM dithiothreitol (DTT), and in ATP-jump experiments, 130 mM NaCl. The experiments were carried out at room temperature (23°C).

To maintain ionic strength in the Na^+ jump experiments, choline chloride was used. The concentration of choline chloride was chosen so that [NaCl] + [ChoCl] was kept constant at a total value given in the corresponding figure captions (100–300 mM).

All chemicals were purchased in analytical grade or higher. In some experiments TRIS buffer was used to exclude an influence of imidazole on the Na^+/K^+-ATPase, but a difference was not detectable.

Solutions containing ATP were made from adenosine-5′-triphosphate disodium salt (Fluka, Neu-Ulm, Germany) in the case of the ATP-jump experiments. In order to avoid Na^+ impurities, for the Na^+ jump experiments adenosine-5′-triphosphate magnesium salt (≈95%, Sigma Aldrich Chem., Deisenhofen, Germany) was used.

For inhibition experiments vanadate (orthovanadate trisodium salt, Na_3VO_4; 99%, Aldrich Chemicals) was prepared as a 30-mM stock solution. Immediately before use an appropriate amount of the stock solution was heated (to dissolve vanadate aggregates), allowed to cool, and added to the buffer solution with a final concentration of typically 1 mM. To avoid Na^+ impurities, vanadate was never added to the nominally Na^+-free solution. The SSM with the protein adsorbed to its surface was incubated in the vanadate-containing solution for at least 10 min. Ouabain-octahydrate with a purity of 95% was purchased from Sigma and added from a 15-mM stock solution.

For the lipid layer diphytanoyl phosphatidylcholine (PC; synthetic; Avanti Polar Lipids Inc., Pelham, AL) and octadecylamine (60:1, wt/wt, 98%, Riedel-DeHaen AG, Seelze-Hannover, Germany) were prepared 1.5% in n-decane according to Bamberg et al., 1979.

Purified membrane fragments (MF) containing Na^+/K^+-ATPase with a protein concentration 2–3 $mg \cdot ml^{-1}$ from the outer medulla of pig kidney were prepared according to Fendler et al., 1985 (modified procedure of Jørgensen, 1974).

Gold electrodes

Glass plates ($7 \times 25\ mm^2$) were cleaned with alcohol and dried. They were brought into the recipient of an evaporation device, which was evacuated to a vacuum pressure of $<1 \cdot 10^{-5}$ mbar. To produce mechanically stable gold layers, the glass surface was covered with chromium (5 nm, Fig. 1) before the gold was deposited (150 nm). The thickness of the material evaporated was measured using a quartz crystal thickness monitor. The desired strip line shape of the gold electrodes was obtained by a 1-mm-thick aluminum mask positioned on the glass substrate before evaporation.

The gold electrodes were incubated in an ethanolic solution of 1 mM octadecyl mercaptan (C_{18}-mercaptan; Aldrich, Steinheim, Germany) for 6 h at room temperature. After mercaptan incubation, the electrodes were rinsed with ethanol, dried, and could be stored dust-free for several days without significant loss of quality. The part of the electrode not designed to act as a membrane electrode, but only as a connecting line, was electrically insulated by covering it with nail polish. Thus the effective membrane areas typically had a width of 1.5 mm and a length of 1–2 mm.

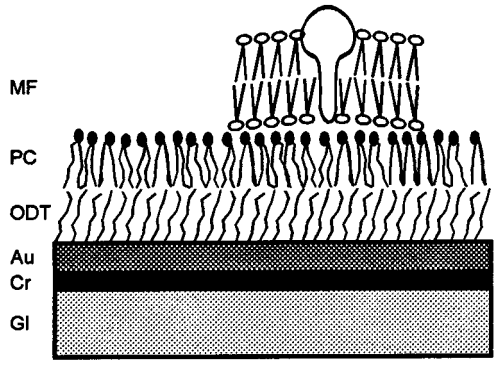

FIGURE 1 Structure of the solid supported membrane (SSM). The SSM consists of a glass support (Gl, 1 mm), a chromium layer (Cr, 5 nm), a gold layer (Au, 150 nm), an octadecyl mercaptan monolayer (ODT), a diphytanoyl phosphatidylcholine monolayer (PC), and the membrane fragments containing the protein (MF).

Cuvettes

To perform rapid concentration jumps, plexiglass cuvettes with an inner volume of 17 μl have been constructed. Between the upper and the lower part of the cuvette, the SSM and an o-ring, which contained the actual reaction volume, were sandwiched. The electrical connection to the membrane electrode was made by a metal plate fixed to the upper part of the cuvette, which was pressed on the SSM, and which was connected to the amplifier. The counterelectrode was an Ag/AgCl electrode divided from the streaming solution by a salt-bridge (polyacrylamide gel). The counterelectrode was mounted on the downstream opening of the cuvette and connected to the electrical circuit.

Setup

A schematic overview of the setup is shown in Fig. 2 *A*. By a perfusor pump (Harvard Pump 22, Harvard Apparatus, South Natick, MA) two 50-ml syringes were driven, which contained the nonactivating and the activating solution, respectively. As both syringes moved simultaneously, each time one solution flowed through the cuvette, the other stream was led into a waste container, and vice versa. This was managed by the special configuration of the electrical 3 × 3 valve (Teflon Valve 360T05, NResearch Inc., Maplewood, NJ; Fig. 2 *B*). To minimize the dead volume between valve and cuvette, the cuvette was positioned close to the front of the valve and connected by a Teflon tubing with an inner diameter of 1 mm. Adding the volumes of cuvette and valve, the dead volume between the point of switching and the membrane sums up to 47 ± 10 μl.

An external connection for cleaning, refilling, and removing bubbles was provided by two 3-way valves between the pump and the electrical valve. All parts of the setup conducting the electrolyte solutions were enclosed in a Faraday cage.

The signal was amplified by an operational amplifier (10^7 V/A, OPA111, Burr-Brown, Tucson, Arizona) located within the Faraday cage and a low noise voltage amplifier (gain: 10^2–10^3). The output signals were filtered (low-pass, 1–10 ms) and recorded. External voltages could be applied to the membrane for determination of membrane conductance and capacitance (see below).

Lipid coating and start of the SSM experiment

The mercaptan-treated gold surface was covered with 4 μl of the lipid solution. During the incubation time of ~1 min the electrode was exposed

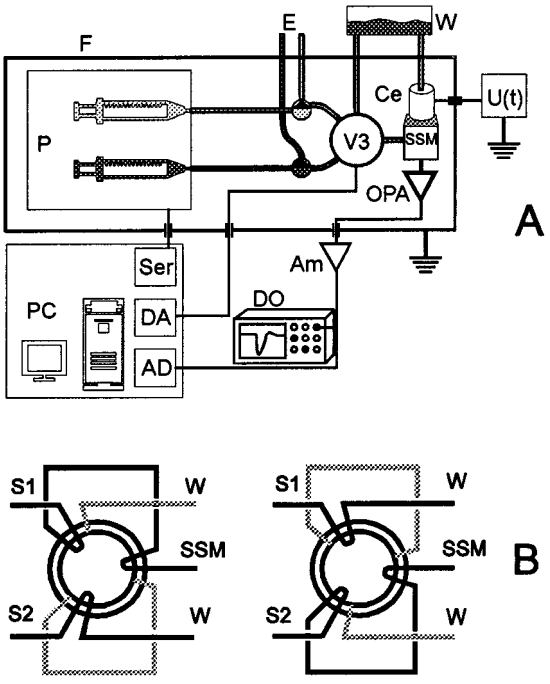

FIGURE 2 (*A*) Experimental setup. The perfusor pump (P), the 3 × 3-way valve (V3), the SSM cuvette (SSM) with the counterelectrode (Ce), and the preamplifier are in a Faraday cage (F). The tubings have an external connection (E). After use the solutions flow into the waste container (W). After filtering and amplification (Am), the time signals are recorded by the digital oscilloscope (DO) and/or the AD converter (AD). Data recording, pump, and electrical valve are controlled by the PC. Capacitance and conductance of the membrane are measured using the voltage source U. (*B*) The configuration of the 3 × 3-way valve in the normal state (*left*) and the activated state (*right*). The black lines represent the pathway of the flowing solutions. The valve is connected to the two syringes (S1, S2), a waste container (W), and the SSM cuvette (SSM).

to air and horizontally oriented. The glass plate was then sandwiched between the upper and lower parts of the cuvette. The effective membrane area was placed under the inlet opening by which the fluid stream was to flow into the cuvette. The cuvette was assembled as shown in Fig. 3 and rapidly filled with the electrolyte solution. The fluid flow was driven by the perfusor pump at maximum pump rate (28 ml/min). Before filling the SSM cuvette, bubbles within the tubings, valves, and syringes of the device had to be carefully removed in order to avoid damage of the SSM surface and perturbations during the experiment.

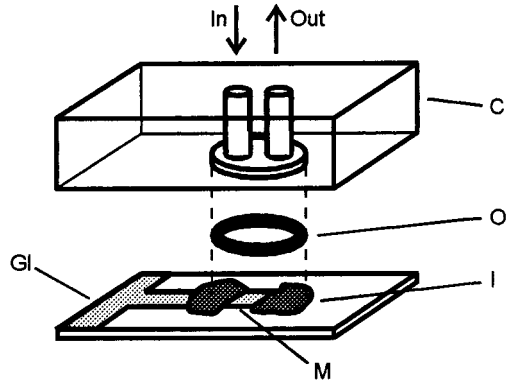

FIGURE 3 Cuvette for rapid solution exchange (not to scale). The letters in the figure denote the SSM glass plate (Gl), the SSM membrane area (M), the electrical insulation (I), the o-ring (O, inner diam. 4.6 mm, height 0.9 mm), and the cuvette (C). The diameter of the solution inlet and outlet (In, Out) is 1 mm.

Measuring procedure, data recording, and analysis

After filling the cuvette with the electrolyte solution, conductance and capacitance of the SSM were monitored by evaluating the current response to a voltage jump (100 mV) and the rectangular response to a triangular voltage (10 mV peak/peak, 0.5 Hz). Because of the polarizability of the gold electrode, the relaxation currents following a voltage jump showed a complicated time dependence. However, the current 1 s after the voltage jump can serve as an arbitrary measure for the conductance (Seifert et al., 1993). After a waiting time of ≈120 min after formation of the SSM, the conductance and capacitance values remained constant at $C = 300-400$ nF/cm^2 and $G_{1s} = 50-100$ nS/cm^2.

At this stage of the procedure we usually performed control experiments with the still protein-free SSM in order to check the signals generated by the solution exchange for artefacts. Especially when large concentration differences were applied (e.g., $\Delta[Na^+] \geq 20$ mM), mixing artefacts were observed. These artefacts could be minimized by replacing the missing electrolyte by a salt, which was assumed not to affect the enzyme (e.g., choline chloride for NaCl). Similarly, activation by smaller amounts of divalent or trivalent ions tended to produce considerable artefacts. For a more detailed discussion on these artefactual currents, see Pintschovius et al., 1999.

The protein was added by injecting 40 μl of a suspension containing 0.2–0.5 mg/ml protein into the cuvette through the outlet channel. The suspension was vigorously mixed using a pipette. The use of 5- to 10-fold lower protein concentrations yielded signal currents, which were not significantly smaller, so the method seems to be useful in cases where only small amounts of purified enzyme are available. The membrane fragments were adsorbed to the SSM during 10 min of waiting time. After control of capacitance and conductance of the compound membrane the experiment was started.

The protocol for a solution exchange (see Fig. 4) typically consisted of four steps: 1) slow cleaning (6 s, 7 ml/min); 2) fast cleaning (2 s, 28 ml/min); 3) activation (concentration jump, 2 s, 28 ml/min); and 4) deac-

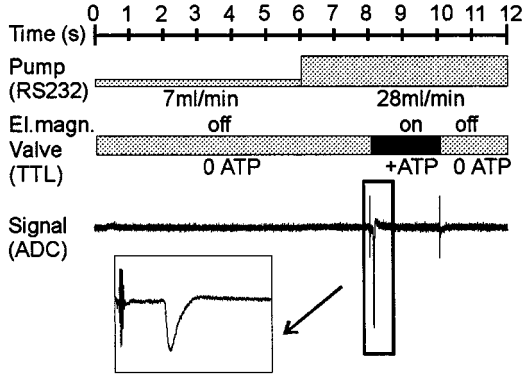

FIGURE 4 Typical time protocol for the electrical measurements. The figure shows the times and flow rates normally used for one concentration jump experiment (here: ATP concentration jump) and the corresponding current signal. In the time trace the switching of the valve shows up as an artefactual current at $t = 8.0$ s and $t = 10.0$ s, respectively. The actual protein current starts ~100 ms after the state of the electrical valve has been changed by a TTL signal. To avoid impurities, the cuvette is cleaned with the nonactivating solution at different flow rates before and after each concentration jump. The flow rate of the perfusor pump is changed via the RS232 interface.

tivation and cleaning (reverse concentration jump, 2 s, 28 ml/min). For reproducible and simple use of the apparatus, the pump, the electrical valve, and data recording were controlled from the PC via our own C/C++ software. The whole procedure was recorded using a 12-bit AD converter at a sampling rate of 1 kHz. Alternatively, and for higher sampling rates, data could be read from a 12-bit digital storage oscilloscope. Data output and input timing were managed by the timer of the AD/DA PC-card (Meilhaus Electronics, Puchheim, Germany). Fitting of the data was performed using the Levenberg-Marquardt least-squares algorithm of the Microcal ORIGIN 3.5 software package (Microcal Inc., Northampton, MA).

RESULTS

Electrical currents generated by the Na$^+$/K$^+$-ATPase were measured by adsorbing Na$^+$/K$^+$-ATPase-containing membrane fragments from pig kidney to an SSM. The ion pumps were activated using a rapid flow technique, which allowed us to generate ATP and Na$^+$ concentration jumps. All experiments presented in this publication were performed in the absence of K$^+$. Under these conditions, dephosphorylation of the enzyme is extremely slow and only the Na$^+$-dependent half of the reaction cycle is investigated.

ATP concentration jump

The Na$^+$/K$^+$-ATPase can be activated either by an ATP concentration jump at constant Na$^+$ concentration or by an Na$^+$ concentration jump at constant ATP concentration. Both procedures have been used, and an ATP and Na$^+$ concentration dependence was determined in each case.

Fig. 5 shows an electrical signal after an ATP concentration jump at a constant Na$^+$ concentration of [Na$^+$] = 130 mM. At $t = 0$ the valve driver is triggered. Switching to the solution containing ATP takes place up to 30 ms later because of electrical and mechanical delay times. At $t \approx$ 130 ms ATP reaches the surface of the SSM corresponding to a transit time of the solution from the valve to the SSM of ~100 ms.

The signal after the ATP jump rises with a time constant of 10 ms and decays with a time constant of ~19 ms. Also, a negative component with a time constant of ~113 ms is observed. As expected, the time dependence of the current is similar to signals obtained on planar membranes using activation with caged ATP (Fendler et al., 1993).

The signals could be completely inhibited by 1 mM orthovanadate. After the measurement of an ATP-induced signal the SSM was incubated with an ATP-free but vanadate-containing solution for ~15 min. Following this procedure, ATP concentration jumps (in the presence of vanadate in both solutions) did not yield any electrical signals. In contrast, inactivation of the ATP-induced signals by ouabain was not possible. This observation is explained by the ouabain being unable to reach its extracellular binding site, which is attached to the SSM surface, and thus not freely accessible from the solution. A similar conclusion was drawn from BLM measurements of Fendler et al., 1985.

Activation of the enzyme with different ATP concentration jumps at constant Na$^+$ concentration of 130 mM is shown in Fig. 6. The peak currents are plotted versus the ATP concentration. As discussed later, the concentration at the surface of the SSM at the time of the peak is less than the nominal concentration in the ATP-containing solution. Therefore, the concentrations have been corrected according to Eq. 4. These values are also included in Fig. 6. A fit to the corrected data with a hyperbolic ATP dependence is shown in the figure and yields a binding constant of 3.0 μM.

The time-dependent current signals at different ATP concentrations were analyzed using a fit with a multiexponential model function. The time constants obtained by the fit are given in Fig. 7. The reciprocal time constant τ_1^{-1} increases, as the substrate concentration is increased without

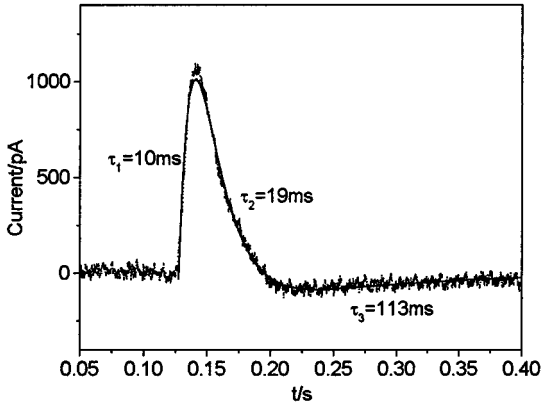

FIGURE 5 Electrical current after an ATP concentration jump. The concentration of ATP in the activating solution was 100 μM. The electrolyte solution contained 130 mM NaCl, 25 mM imidazole, 3 mM $MgCl_2$, and 0.2 mM DTT at pH 7.0 (HCl). The temperature during the experiments was 22°C. The parameters of the fitted curve (sum of three exponentials, *solid line*) are: $A_1 = -4530$ pA, $\tau_1 = 10$ ms, $A_2 = 5030$ pA, $\tau_2 = 19$ ms, $A_3 = -260$ pA, $\tau_3 = 113$ ms.

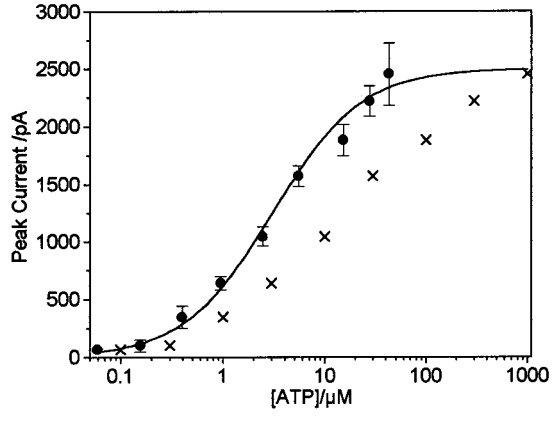

FIGURE 6 ATP dependence of the peak currents after an ATP concentration jump experiment. The electrolyte solution contained 130 mM NaCl, 25 mM imidazole, 3 mM $MgCl_2$, and 0.2 mM DTT at pH 7.0 (HCl). The experiments were performed at 22°C. The peak currents are plotted versus the corrected (*circle*) and the uncorrected (*cross*) concentrations, respectively. Data fitting of the corrected values with a Michaelis-Menten function and $I_{peak,max} = 2500$ pA gave $K_M = 3.0$ μM.

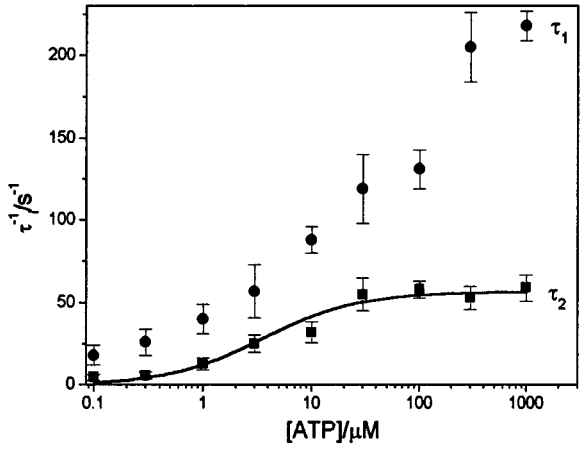

FIGURE 7 ATP concentration jumps (data sets identical to Fig. 6). The concentration dependence of the signal rise and decay rates τ_1^{-1} (*circles*) and τ_2^{-1} (*rectangles*) is shown. The half-saturating concentration value of τ_2^{-1} is $K_M = 3.4$ μM, the maximum rate 60 s^{-1} (*solid line:* Michaelis-Menten fit).

showing saturating behavior. The reciprocal time constant of the decay (τ_2^{-1}) also increases with [ATP]. In contrast to τ_1^{-1} it saturates at high ATP concentrations with half-saturating [ATP] of $K_M = 3.4$ μM and a maximum rate of $\tau_{2,max}^{-1} = 60$ s^{-1}.

This K_M value is in good agreement with the value obtained for the saturation of the peak current of the signal (3.0 μM, Fig. 6). The agreement is not unexpected, since in the absence of K^+ the ion pump performs only a single turnover. As the charge transported during the turnover is constant, the integration of the electrical current yields a constant, which implies that the ratio of amplitude and reciprocal time constant is a constant.

In a third phase of the time course the current signal changes its sign. The corresponding rate constant τ_3^{-1} is ~8 s^{-1}. This phase of the signal corresponds to the discharge of the capacitances of the membrane system (see Discussion).

Peak currents after activation of the enzyme with a 100-μM ATP concentration jump at different Na^+ concentrations are shown in Fig. 8. Concentration correction was not necessary in this case, since the Na^+ concentration was constant during a single experiment. The model function used for fitting the [Na^+] dependence of the peak currents I_{peak}^{max} was a Hill function with a Hill coefficient n and a half-saturation concentration $K_{0.5}^{Na}$. I_{peak}^{max}, $K_{0.5}^{Na}$, and n were adjustable parameters during the fitting procedure:

$$I_{peak} = \frac{I_{peak}^{max}}{1 + (K_{0.5}^{Na}/c_0)^n} \quad (1)$$

Fits using (fixed) $n = 1$ (Michaelis-Menten kinetics) did not yield acceptable results. Good fits were obtained with a Hill coefficient $n = 2.4$ and a binding constant of $K_{0.5}^{Na} = 2.6$ mM.

Na^+ concentration jump

Fig. 9 shows an electrical signal after a Na^+ concentration jump of 100 mM at a constant ATP concentration of 100 μM. A transit time of the solution from the valve to the SSM of ~100 ms is obtained which is similar to the value in the case of the ATP concentration jump. The phase of decay and subsequent phase with negative current are described by the rate constants 63 and 30 s^{-1}. A multiexponential fit also including the rising phase did not give reasonable results. As in the case of the ATP concentration jumps, the signal could be inhibited by preincubating the membranes with 1 mM orthovanadate.

Fig. 10 shows the peak currents obtained using different Na^+ concentration jumps at a constant ATP concentration

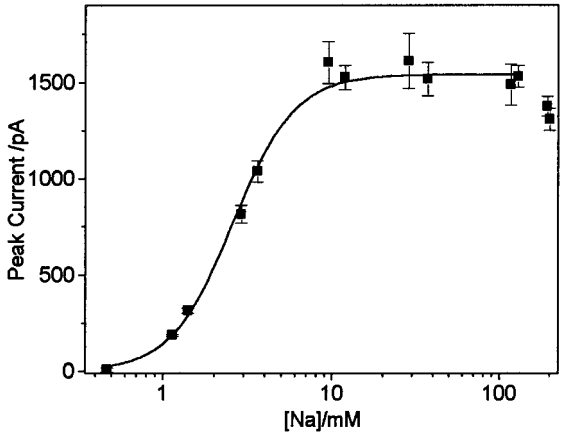

FIGURE 8 Na^+ dependence of ATP concentration jump experiments (Δ[ATP] = 100 μM). No correction of the concentration values was necessary in this mode of concentration-dependent measurement. The solution contained x mM NaCl, 200 − x mM choline chloride, 25 mM imidazole (pH 7.0, HCl), 3 mM $MgCl_2$, and 0.2 mM DTT at 22°C. The best fit was obtained with a Hill equation using a Hill exponent $n = 2.4$ and a half-maximal concentration $K_{0.5}^{Na} = 2.6$ mM.

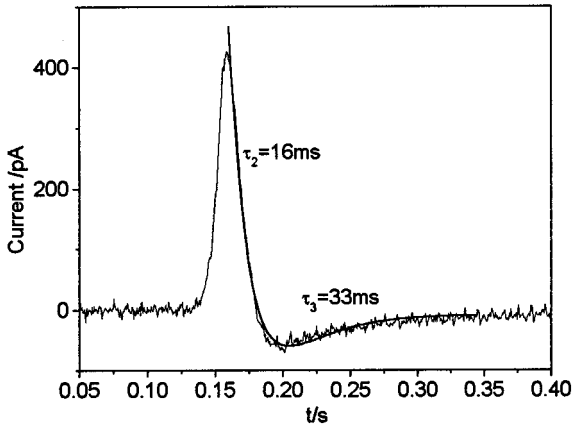

FIGURE 9 Electrical signal after a 100 mM Na^+ concentration jump. Conditions: 300 mM choline chloride or 200 mM plus 100 mM NaCl, 25 mM imidazole, 0.2 mM DTT, 3 mM $MgCl_2$, pH 7.0 (HCl), 25°C. The data set could not be fitted by a multiexponential fit including the rising phase of the signal. A biexponential fit of the signal phases following the peak yields time constants of 16 and 33 ms, respectively (62 s^{-1} and 30 s^{-1}).

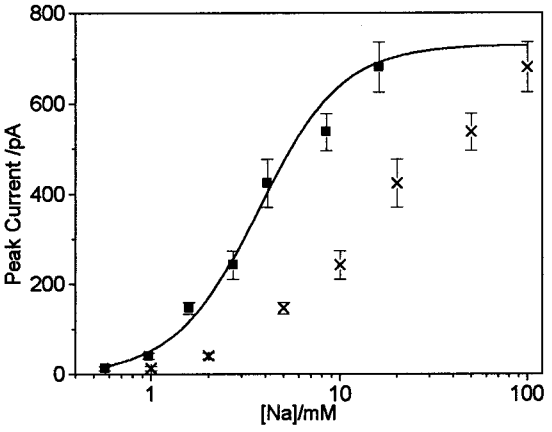

FIGURE 10 Na^+ dependence of the Na^+ concentration jump experiments. The electrolyte solution contained 25 mM imidazole, 3 mM $MgCl_2$, 0.2 mM DTT, and 100 μM ATP at pH 7.0 (HCl). The nonactivating solution contained 300 mM choline chloride, whereas the activating solution contained varying Na^+ concentrations plus the amount of choline chloride required to yield total salt concentration of 300 mM. The experiments were performed at 22°C. The peak currents are plotted versus the corrected (*square*) and the uncorrected (*cross*) concentrations, respectively. Fitting of the corrected data with a Hill function gave acceptable results only for $n = 2$. With $I_{peak,max} = 750$ pA $K_M = 3.7$ mM was obtained.

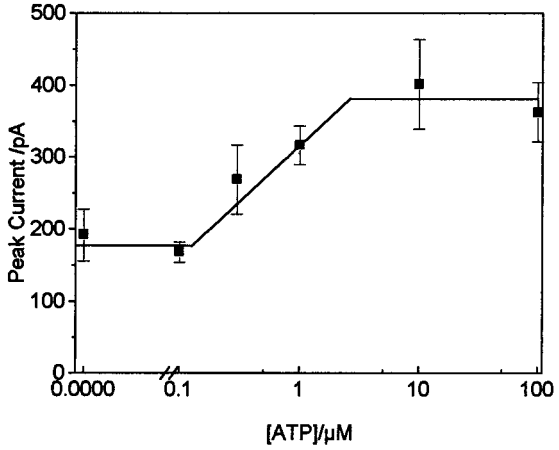

FIGURE 11 ATP dependence of the Na^+ concentration jump experiments. The electrolyte solution contained 110 mM choline chloride, 25 mM imidazole, 3 mM $MgCl_2$, 0.2 mM DTT, and varying amounts of ATP at pH 7.0 (HCl). The activating solution contained 100 mM choline chloride plus 10 mM NaCl instead of 110 mM choline chloride. The experiments were performed at 22°C. The peak currents are evaluated versus the ATP concentration. At [ATP] = 0 a finite signal amplitude is obtained due to electrogenic Na^+ binding. The half-maximal increase of the peak amplitudes takes place at [ATP] $\approx$ 1 μM.

of 100 μM. The concentration values had to be corrected (cf. Fig. 6) according to Eq. 4. In the figure the uncorrected and the corrected data points are shown together with a fit for the corrected points. Also in this case a Hill coefficient $n > 1$ was required. A good fit with n as an adjustable parameter could be obtained yielding a Hill coefficient of $n = 2.0$ and a half-saturation of 3.7 mM. No acceptable fit was obtained using fixed $n = 1$. This agrees well with the value of $K_M^{Na} = 2.6$ mM obtained from the data shown in Fig. 8.

An Na^+ jump experiment with variable ATP concentration is shown in Fig. 11, where the peak amplitudes of the current signals were evaluated. The concentration amplitude chosen for Na^+ activation was 10 mM. The most striking feature of the plot is the finite signal amplitude at vanishing ATP concentration, suggesting electrogenic binding of Na^+ to the enzyme in the absence of ATP. Note that a contamination of the preparation with ATP can be ruled out because the buffers used for the Na^+ jumps were all ATP-free. At the flow rate used in the experiments (28 ml/min) the cuvette volume is exchanged ~13 times during each experiment, washing out all possible contaminants.

An increase in [ATP] leads to larger peak currents (binding constant of $K^{ATP} \sim 1$ μM). This demonstrates that Na^+ activation in the absence of ATP can yield information about the electrogenicity of Na^+ binding steps in the transport cycle of the Na^+/K^+-ATPase. We will discuss that separately in a subsequent publication (Pintschovius et al., 1999).

Correction of concentration values

As will be discussed in more detail below, two effects dominate the time for the activating solution to reach the electrode and the steepness of the concentration step: a boundary layer effect on the electrode surface and the fluid dispersion in the tubings (i.e., stream velocity is not constant within the tubings). For the correction of the concentration values we use for simplicity the functional dependence derived for laminar Hagen-Poiseuille flow in a cylindrical tubing. However, to account for all effects contributing to the rise of the concentration step at the electrode surface, an empirical parameter τ_{app} is included as shown below.

Assuming laminar Hagen-Poiseuille flow in a cylindrical tubing, the average concentration $c(t)$ at the position of the membrane rises according to (see Appendix):

$$c(t) = \begin{cases} c_0[1 - (t_0/t)] & \text{for} \quad t \geq t_0 \\ 0 & \text{for} \quad t < t_0 \end{cases} \qquad (2)$$

where t_0 is a function of the distance between the membrane and the valve (see Appendix). Calculations with typical parameters of our setup yield $t_0 = 51 \pm 11$ ms (taking into account the dispersion effect only). It represents at the same time the time constant describing the steepness of the concentration step as well as the transfer time of a molecule moving on the fastest (central) streamline from the valve to the electrode. This means that the first activating molecules reach the protein at time t_0, and the concentration starts rising. After the time $t_0 + t_{peak}$ the maximum current is observed. As the concentration is rising slowly (usually t_{peak} is less than the steepness t_0), at this time the concentration c on the membrane surface has not reached its full value c_o. This implies the need for correcting concentration values of the activating substance.

Now the risetime t_0 is replaced by an empirical parameter τ_{app} that will be determined using experimental data:

$$c(t) = \begin{cases} c_0[1 - (\tau_{app}/t)] & \text{for} \quad t \geq \tau_{app} \\ 0 & \text{for} \quad t < \tau_{app} \end{cases} \tag{3}$$

Here $t = 0$ represents the time when the valve is switched. Especially at the time of the current peak t_{peak}, the concentration is

$$c_{peak} = c_0\left(1 - \frac{\tau_{app}}{t_{peak}}\right). \tag{4}$$

In order to obtain phenomenological values for τ_{app}, the ATP-jumps at varying ATP values c_0 from Fig. 6 were evaluated. From this dataset peak currents I_{peak} and times t_{peak}, at which the peak was reached, were determined for ATP concentration values c_0 between 0.1 and 1000 μM. For each [ATP] value six concentration jumps were evaluated yielding averages for $\bar{I}_{peak}$ and $\bar{t}_{peak}$ with their standard deviations. It was assumed that the dependence is ideally represented by a Michaelis-Menten curve with half-saturating concentration K_M:

$$I_{peak} = \frac{I_{peak}^{max}}{1 + K_M/c_{peak}} = \frac{I_{peak}^{max}}{1 + K_M \Big/ \left[c_0\left(1 - \frac{\tau_{app}}{t_{peak}}\right)\right]} \tag{5}$$

where I_{peak}^{max} denotes the peak current at saturating substrate concentrations.

The data $\bar{I}_{peak}(c_0, \bar{t}_{peak})$ were fitted (Fig. 12) using this equation at a fixed $I_{peak}^{max} = 2500$ pA. Different K_M between 2 and 8 μM were chosen and fixed during each fit procedure. Thus, the only adjustable parameter of each individual fit was τ_{app}, which is plotted together with the corresponding reduced sum of squares χ^2 in Fig. 12 (Fendler et al., 1993; Bevington, 1969). Minimum χ^2_{min} was encountered at $K_M = 3.0$ μM. The confidence interval (68%) is determined by $\chi^2_{min} + 1$ (Bevington, 1969) and gives a range of 2.3–4.1 μM. The fitted τ_{app} was 89 ms for $K_M = 3.0$ μM. The confidence interval for τ_{app} was between 81 and 91 ms.

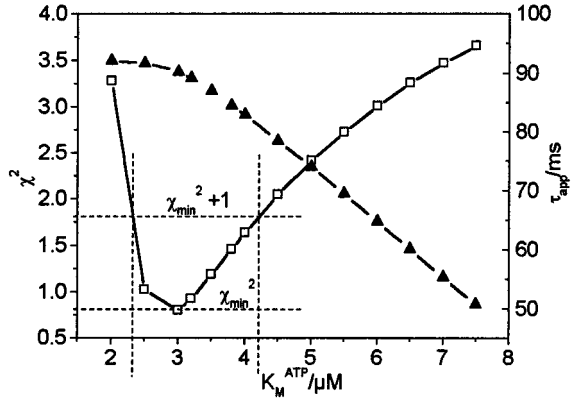

FIGURE 12 Evaluation of peak currents $I_{peak}(c_0, t_{peak})$ after ATP-jumps with c_0 = [ATP]. The concentration rise time τ_{app} (*triangles*) was fitted using the model function Eq. 5 and different (but fixed) K_M from 2 to 8 μM and the reduced sum of squares χ^2 was calculated. The minimum χ^2 (*open squares*) was found for $K_M = 3.0$ μM and $\tau_{app} = 89$ ms.

The ATP-affinity obtained by this evaluation is compatible with earlier measurements performed with caged ATP at lipid bilayer membranes under similar conditions (Nagel et al., 1987: 2 μM), and with the [ATP]-dependence of the rates τ_2^{-1} determined from the same dataset in this publication using uncorrected concentrations (3.4 μM). Moreover, the prediction of $t_0 = \tau_{app}$ ($t_0 \sim 100$ ms) is shown to be valid not only for flow through the tubes, but approximately also for fluid transport as a whole.

DISCUSSION

A new technique

Electrical currents generated by the Na^+/K^+-ATPase were measured by adsorbing Na^+/K^+-ATPase-containing membrane fragments to a solid supported membrane (SSM). This preparation has been introduced recently using a number of different electrogenic ion pumps (Seifert et al., 1993). The SSM acts as a carrier for the membrane fragments and as a high-capacitance, low-conductance electrode. In the previous study (Seifert et al., 1993) a photolabile substrate (caged ATP) was used to generate a rapid ATP concentration jump. Here we describe a flow injection technique that allows us to generate concentration jumps with virtually any substrate.

If substrates are applied that are not available as a caged compound, this new technique has been demonstrated to be useful. It combines the advantages of rapid flow methods with those of recording electrical currents, thus providing a novel tool for the investigation of electrogenic reaction steps in the transport pathway of ion-translocating membrane proteins. For the first time currents generated by electrogenic Na^+ binding to the cytoplasmic membrane surface of the Na^+/K^+-ATPase under ATP-free conditions could be observed. This will be presented in more detail in a subsequent publication.

Another advantage of the method is the stability of membrane preparations, so that the protein can be investigated during hours under many different conditions with the same preparation. The conditions can be changed arbitrarily, i.e., it is possible not only to add a certain substance, but also to remove it. The amount of protein required for an experiment is very small, as the membrane fragments or vesicles containing the enzyme keep being adsorbed during the whole lifetime of the SSM. Forty μl of a suspension containing only 0.1 mg/ml of protein (5 μg) are sufficient to generate a signal as large as 75% of the values obtained under standard experimental conditions (~0.5 mg/ml, see Fig. 5).

In contrast to other SSM techniques (for a review see Xu and Li, 1995) the simplicity of preparation of the self-assembled octadecyl mercaptan monolayer on gold together with the high electrical resistance of the mercaptan/lipid bilayer makes this technique attractive for the investigation of currents generated by a broad spectrum of ion transporters.

The replacement of one buffer by another buffer of different composition can yield electrical artefacts caused by the change in concentration and type of ions, which undergo unspecific binding processes at the membrane surface. This limitation is generally inherent to methods based on solution exchange. Such artefactual currents, which are independent of the presence of protein, are difficult to circumvent and can only be minimized by the appropriate choice of solutes.

For the solution exchange at the surface a time resolution of $\tau_{app} = 89$ ms was obtained. This value has been experimentally determined from the concentration dependence of the Na$^+$/K$^+$-ATPase pump currents. The value of τ_{app} cannot be identified with the time resolution of the observed current curves, as the use of supersaturating concentrations leads the protein into saturation after significantly shorter times. Thereby risetimes for the pump currents as low as 10 ms and smaller could be obtained (see τ_1^{-1} in Fig. 7).

The time resolution is determined by the switching time of the valve, fluid dispersion within the volume between the valve assembly and the SSM-cuvette, and the transfer processes in the reaction volume including the presence of an unstirred boundary layer at the surface of the SSM. In the following section the contributions of the different processes to time resolution are estimated. This information can help to shorten the risetime of the concentration at the SSM surface by appropriate constructive improvements of the instruments.

Further improvements for shortening the time necessary for solution exchange are presently under development. The strategy implies an increase in flow velocity of the fluid stream as well as a minimization of the volume between the location of switching and the membrane surface.

Time resolution of the instrument

Measurements that are dependent on a rapid exchange of fluids on a surface usually have a limited time resolution. Especially when objects larger than a few micrometers are to be investigated, time-resolved measurements in the millisecond range become difficult because of unstirred layer effects. In the following we give a semiquantitative account of several effects that slow the risetime of the concentration jump performed at the surface of the SSM. This risetime of the apparatus will be referred to as τ_{app}.

There are at least four effects that considerably contribute to the limited time resolution of the concentration step at the membrane surface: 1) the switching of the electrical valve; 2) the dispersion of the concentration step in the tubing connecting the valve with the reaction chamber; 3) the mixing and the transport within the reaction volume; and 4) the formation of an unstirred boundary layer at the SSM, where transport across this layer is assumed to take place by diffusion only. In the following, we estimate the contributions of the different effects.

The switching time of the electrical valve (1) is between 5 and 15 ms. Fluid dispersion in the tubing (2) is due to the radially inhomogeneous velocity distribution. The time constant t_0 that can be calculated from the velocity distribution of a laminar fluid stream in a cylindrically shaped channel (Hagen-Poiseuille law; see Appendix, Eq. 17), is the risetime of the mean concentration (average over all streamlines) after passing the volume (V_T) between the valve and the reaction chamber. One obtains $t_0 = V_T/2\dot{V} = 51 \pm 11$ ms ($\dot{V} = 28$ ml/min, $V_T = 47 \pm 10$ μl).

A detailed knowledge of the three-dimensional velocity distribution within the reaction volume (3) is difficult to acquire. A simple model will be treated below. Unstirred layer effects (4) often present a serious problem when dealing with transport through membranes (for a review on this topic see Barry and Diamond, 1984). Values for boundary layer thicknesses generally depend on the stirring rate, i.e., velocity of the fluid in the bulk solution, and the area of the object under consideration. Typical experimental thickness values (examples given in Barry and Diamond, 1984) vary in a wide range between <1 μm (stopped flow with erythrocytes) and hundreds of micrometers (biological tissue samples under slow stirring). Theoretically, the boundary layer thickness δ can be estimated from the knowledge of the parameters of the hydrodynamic problem.

In almost all practical cases an exact calculation of the transport process through the boundary layer is impossible. Therefore, we suggest a simplified model (Fig. 13) in order to estimate the order of magnitude of effects (3) and (4). We assume that the reaction volume represents a channel of width w and height h, where $w \gg h$. In such a channel, the velocity distribution $u(y)$ with $-h/2 < y < h/2$ behaves like (Bensimon et al., 1986)

$$u(y) = \frac{3(h^2 - 4y^2)}{2wh^3}\dot{V} \qquad (6)$$

The transfer process consists of two contributions, namely of a) transport within layer y of the fluid flow along a

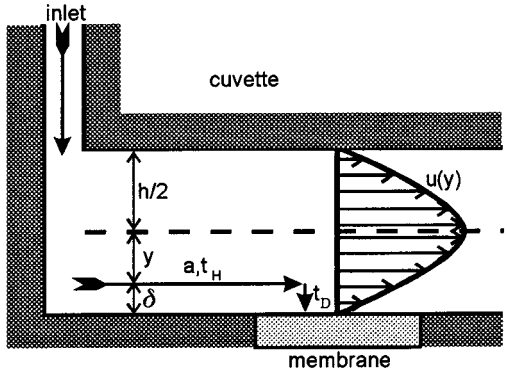

FIGURE 13 Simplified model for the estimation of the transfer time from the inlet opening to the membrane surface. It is assumed that the solution is transported in two steps, the first one dominated by the movement within the fluid stream (t_H) over a distance a, and the second one dominated by diffusive transport through a boundary layer of thickness δ (t_D). A parabolic velocity profile $u(y)$ in a channel (width w, height h) is assumed.

distance a, and of b) diffusional transport across the boundary layer of thickness $\delta = h/2 - y$ (Fig. 13).

The time t_H required for hydrodynamic transport with velocity $u(y)$ is

$$t_H = a/u(y) = \frac{2awh^3}{3(h^2 - 4y^2)\dot{V}} \quad (7)$$

During this time interval substrate ions can diffuse toward the electrode. The diffusion through the layer of thickness $\delta = h/2 - y$ takes the time t_D (rise time, after which half of the maximal concentration is reached; Barry and Diamond, 1984):

$$t_D = 0,38\delta^2/D \quad (8)$$

On a streamline at distance δ from the membrane, for which the two time intervals are equal ($t_H = t_D$), and with $\delta \ll h$ one calculates:

$$\delta^3 = 0,439 \cdot \frac{awh^2D}{\dot{V}} \quad (9)$$

In our case, typical values $a = 1$ mm, $w = 3$ mm, $h = 0.8$ mm, $D_{ATP} = 3 \cdot 10^{-4}$ mm^2/s, and $\dot{V} = 28$ ml/min $= 520$ mm^3/s yield

$$\delta = 7.9\ \mu\text{m} \quad (10)$$

For the transfer times one obtains

$$t_H = t_D = 78\ \text{ms} \quad (11)$$

Compared to the experimentally determined value for the total of all effects limiting the time resolution (89 ms), the sum of values for the single effects 2 (51 ms) and 3 & 4 (78 ms) based on the simple models is too large. As the velocity distribution within the cuvette is highly inhomogeneous, δ, and at the same time the risetime of the concentration, are expected to vary locally, so that for an SSM surface at a location with high fluid velocity a thinner boundary layer δ, and thus also smaller contributions for the risetime, are expected. For the construction and optimal adjustment of the SSM this implies that the membrane area should be as small as possible (to minimize variation of δ) being located under the inlet opening of the reaction volume (to maximize fluid velocity).

The boundary layer contributes significantly to the time resolution. At the same time it is useful for measurements at relatively high flow rates: the boundary layer having dimensions in the order of micrometers is much thicker than the membrane fragments and thus prevents the fragments from being dragged away with the flow. Our experience shows that the preparation is indeed very stable, and even flow rates four times higher than applied in the experiments presented here never did cause any detectable loss of protein from the SSM surface.

Although the rise time of the substrate concentration at the SSM surface is ~90 ms, signal kinetics of ATP activation of the Na^+/K^+-ATPase were measured with a time resolution of 10 ms if ATP was added at an oversaturating substrate concentration (see Fig. 5). In this case, the substrate binding site is saturated after a much shorter time than the time required for a complete solution exchange. This enables measurements with high time resolution under the constraint that the enzyme can only be investigated under saturating conditions.

Electrogenic Na^+ translocation by the Na^+/K^+-ATPase

Electrogenic Na^+ translocation in the Na^+/K^+-ATPase could be demonstrated after an ATP or a Na^+ concentration jump. The sign of the electrical currents corresponds to the transport of positive charge from the aqueous medium to the SSM. From the direction of the current we conclude that the Na^+/K^+-ATPase membrane fragments contributing to the signal current are adsorbed with their extracellular side facing the SSM. The same conclusion was drawn from inhibition experiments with ouabain and orthovanadate (Pintschovius et al., 1999).

Artefactual response of the apparatus due to the rapid solution exchange at the SSM surface was ruled out by control experiments without protein and by inhibition with orthovanadate. The characteristics of the measured signals under various conditions are now discussed. The comparison of ATP and Na^+ jump experiments serves as an internal consistency check of the system.

Because of the limited risetime τ_{app} of the concentration at the SSM surface, the Na^+ and ATP concentration dependencies in Fig. 6 and Fig. 10 have to be corrected. The correction procedure is based on the fact that at the time when the current reaches its peak, the concentration has not yet reached its final value (see Results). If the concentration dependence is determined for a substrate that is different from the substrate responsible for the concentration jump, then of course no such correction is necessary. The latter is the case for Na^+ jumps at variable ATP concentration or ATP jumps at variable Na^+ concentration.

The validity of the correction procedure is demonstrated by the similar values of $K_{0.5}^{Na}$ obtained with ATP and Na^+ concentration jumps (Fig. 8, 2.6 mM; Fig. 10, 3.7 mM). This comparison is not possible for K_M^{ATP} in Fig. 6 and Fig. 11 because the ATP affinity of the Na^+/K^+-ATPase depends on the Na^+ concentration, which was not saturating in Fig. 11.

From BLM measurements using caged ATP an Na^+ binding constant $K_{0.5}^{Na} = 3$ mM (Nagel et al., 1987) was obtained, which is obviously in good agreement with the values determined by rapid solution exchange presented here ($K_{0.5}^{Na} = 2.6$ mM and 3.7 mM for ATP-jumps and Na^+-jumps, respectively). The concentration dependence of Na^+ and ATP concentration jumps shows cooperative Na^+ binding with a Hill coefficient of 2.0–2.4. This in good agreement with data reported for the cytoplasmic Na^+ bind-

ing site (Goldshleger et al., 1987) of $K_{0.5}^{Na} = 3–7$ mM and Hill coefficient 1.8–1.9.

Time dependence of the electrical currents

As mentioned above, at high substrate concentrations a high time resolution (<10 ms) comparable to that of bilayer measurements using caged ATP (Fendler et al., 1987; Borlinghaus et al., 1987) can be obtained. At low substrate concentrations, however, the risetime of the concentration at the surface of the SSM may be considerable, determining the time dependence of the measured current. Therefore, we have quantitatively evaluated the electrical signals at various ATP concentrations using a multiexponential fitting procedure. This is compared to a numerical simulation that includes the effect of substrate concentration being time-dependent (see Appendix).

In this respect it has to be noted that our data could not be fitted by a sum of exponential functions under all conditions. This behavior is explained by the rather slow increase in substrate concentration, which leads to a slowly rising phase of the measured currents. As the substrate concentration $c(t)$ at the membrane surface varies in time, the pseudo-first-order binding rate "constant" $k_{ATP}^{+} \cdot c(t)$ becomes time-dependent, and thus a multiexponential time behavior can no longer be expected. In cases where multiexponential curve-fitting was impossible, the fitting procedure was restricted to the data following the current peak.

The reciprocal time constant of the rising phase (τ_1) is strongly dependent on substrate concentration (Fig. 7). It increases as c_0 is increased and does not saturate in the concentration range up to 1 mM ATP. In a previous paper (Fendler et al., 1987) τ_1^{-1} was found to be independent of ATP concentration and was assigned to the rate constant of electrogenic Na^+ translocation in the Na^+/K^+-ATPase reaction sequence. The behavior of τ_1 is obviously different in the case of the rapid flow technique presented here. The reason for this difference is that in Fendler et al. (1987) caged ATP was used for the activation of the enzyme, which is a competitive inhibitor of ATP. This limits the pseudo-first-order rate constant of ATP binding to values below $\sim 30\ s^{-1}$, which is smaller than that of Na^+ translocation. Therefore, τ_1 corresponds to the Na^+ translocation step at all ATP concentrations. In contrast, the data shown in Fig. 7 were obtained in the absence of caged ATP. At ATP concentrations $\gtrsim 10\ \mu M$, the pseudo-first-order rate constant of ATP binding becomes larger than that of Na^+ translocation. In consequence, the ATP-dependent reaction appears in the rising phase of the signal (τ_1) at high ATP concentrations.

After reaching its maximum value, the current induced by the ATP concentration jump (Fig. 5) decays with a time constant $\tau_2 = 19$ ms; τ_2^{-1}, as τ_1^{-1}, increases with the ATP concentration c_0 but, in contrast, saturates at $60\ s^{-1}$. In fact, saturation is expected at the rate constant of the rate-limiting electrogenic reaction following ATP binding ($E_1ATP \rightarrow E_2P$). Similarly, a time constant $\tau_2^{-1} \approx 60\ s^{-1}$ is obtained after a 100-mM Na^+ concentration jump. For a more detailed discussion see our numerical simulation below.

The slowest time constant, τ_3, having a negative signal amplitude has previously been interpreted as the time constant of the reflux from the electrically charged capacitance of the compound membrane. Transient current kinetics of the Na^+/K^+-ATPase in the absence of K^+ yield $\tau_3^{-1} = 2.9\ s^{-1}$ (Fendler et al., 1987). At the SSM (Seifert et al., 1993) using caged ATP $\tau_3^{-1} = 1.3\ s^{-1}$ was determined in the absence of K^+. These values are relatively small compared to our $\tau_3^{-1} = 8.8\ s^{-1}$ (ATP concentration jump) and $\tau_3^{-1} = 30\ s^{-1}$ (Na^+ concentration jump). The discrepancy could be related to different adsorption conditions leading to a different membrane conductance G_m, and thus to a change in the rate of discharge of the membrane fragments. Also, it has been speculated that the protein is involved in the discharge kinetics (Fendler et al., 1993), which would explain the variation of τ_3^{-1} under different conditions.

Simulation of the electrical current

One major aim of this study was to perform pre-steady-state experiments in order to collect information about the rate constants of certain reaction sequences. How does the relatively large risetime of the concentration step at the surface of the SSM influence the time-dependence of the current response? We have simulated our ATP jump measurements (Figs. 14 and 15) by the following model:

$$ATP + E_1 \underset{k_{ATP}^{-}}{\overset{k_{ATP}^{+}}{\rightleftharpoons}} E_1ATP \overset{k_2}{\rightharpoonup} E_2P \qquad (12)$$

This model includes 1) a time-dependent ATP concentration $c(t)$, where $c(t)$ is represented by the model function derived for tube dispersion (Eq. 3 with rise time τ_{app}); 2) an ATP binding process with a second-order forward binding rate k_{ATP}^{+} and a backward rate k_{ATP}^{-}; 3) subsequent electrogenic single-turnover Na^+ translocation with rate k_2; and 4) discharge of the membrane capacitance with time constant τ_0. The set of equations used for the numerical simulation is shown in the Appendix. The parameters used for the simulation shown in Fig. 14 were $k_{ATP}^{+} = 30 \cdot 10^6\ M^{-1}\ s^{-1}$, $k_{ATP}^{-} = 90\ s^{-1}$, $k_2 = 60\ s^{-1}$, and $\tau_{app} = 89\ s^{-1}$.

For an ideal concentration step ($\tau_{app} = 0$), the set of equations is solved by a sum of three exponential functions. In the case of finite values of τ_{app} the solution of the problem is no longer a sum of three exponentials. Nevertheless, the simulated curves can be fitted approximately by a triexponential model function yielding the reciprocal time constants τ_1^{-1}, τ_2^{-1}, and τ_3^{-1}.

The time-dependent currents obtained from the numerical simulation at different ATP concentrations are shown in Fig. 14 *A*. To these curves a triexponential function was fitted. This procedure yielded three time constants (τ_1, τ_2, and τ_3). The current component with time constant τ_3 has a

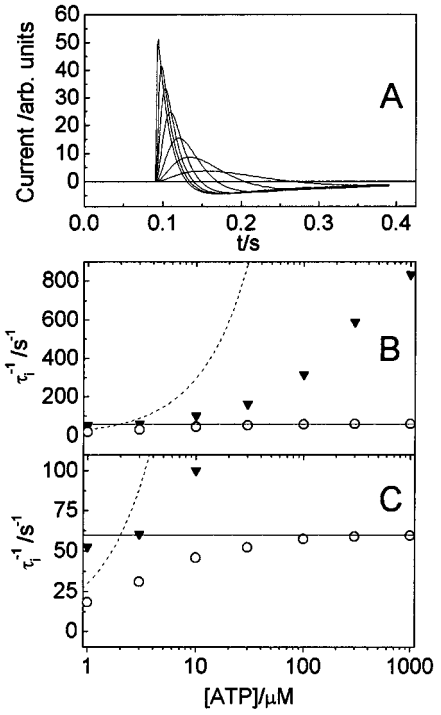

FIGURE 14 (*A*) Simulation of data with a slow concentration rise (89 ms) according to Eq. 21 at ATP concentrations 0.3, 1, 3, 10, 30, 100, 300, and 1000 μM. (*B*) The signal rise and decay rates τ_1^{-1} (*triangles*) and τ_2^{-1} (*circles*) were determined from the time course of the simulation (*A*) as described in the text. The dashed line corresponds to the quasi-first-order rate of ATP binding $k_{ATP}^{+} \cdot c_0$, the solid line to the rate constant of Na^+ translocation k_2. (*C*) Same data as (*B*) but with different scaling.

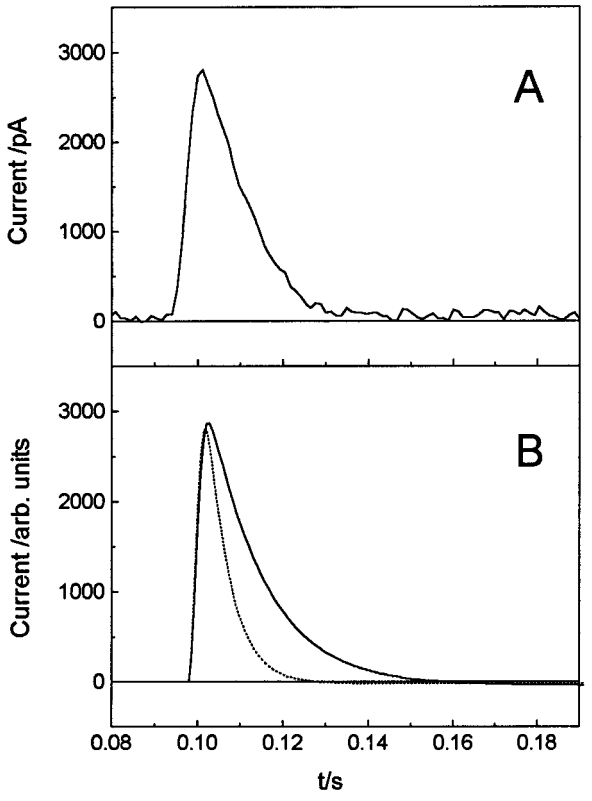

FIGURE 15 ATP concentration jump (1 mM): experimental data (*A*) and simulations (*B*) using parameter values from the text. A simulation (for a concentration rise time of 89 ms) with $k_2 = 200\ s^{-1}$ (*dotted line*) is not able to reproduce the data, whereas $k_2 = 80\ s^{-1}$ (*solid line*) gives a good approximation of the real data.

negative amplitude and is a result of the capacitive coupling of the membrane fragments. τ_3 is not relevant from a kinetical viewpoint and will not be discussed further. The ATP concentration dependence of τ_1^{-1} and τ_2^{-1} is shown in Fig. 14, *B* and *C*, both showing the same data, but at different scaling.

Fig. 14, *B* and *C* also include the pseudo-first-order rate constant of ATP binding $k_{ATP}^{+} \cdot c_0$ (*dashed line*) where c_0 is the ATP concentration and k_{ATP}^{+} is the second-order rate constant for ATP binding. Obviously, at ATP concentrations above 2 μM, the values of the curve $k_{ATP}^{+} \cdot c_0$ are greater than any of the time constants determined from the simulation. This demonstrates that under these conditions the saturation of the ATP binding sites is slowed by the slow risetime τ_{app} of the ATP concentration.

Following the arguments given above and considering the kinetic model, we expect two time constants: one of ATP activation, which depends on ATP concentration, and one of Na^+ translocation determined by k_2, which does not. This seems to disagree with the data of Fig. 14, *B* and *C*. The apparent contradiction is brought about by the fact that the time constants shown in the figure are labeled in the order of their magnitude rather than according to the underlying process. Below ~3 μM, τ_1 has to be assigned to the ATP-independent reaction $E_1ATP \rightharpoonup E_2P$ and τ_2 to ATP activation. Above 3 μM τ_1 is determined by ATP activation and τ_2 by $E_1ATP \rightharpoonup E_2P$. Accordingly, the reciprocal time constant corresponding to the rate constant $k_2 = 60\ s^{-1}$ determines τ_1 below 3 μM and τ_2 above. A corresponding argument can be given for the time constant of ATP activation. The fact that τ_1^{-1} and τ_2^{-1} are both determined by k_2 but in different concentration ranges is illustrated by the straight line in Fig. 14 *B*, which corresponds to $k_2 = 60\ s^{-1}$. Note that the saturation value of τ_2^{-1} gives the rate constant k_2 of Na^+ translocation.

The qualitative behavior of the simulated rates (Fig. 14) is similar to that of the observed rates (Fig. 7). For the simulation a time constant of the apparatus $\tau_{app} = 89$ ms—as determined experimentally—was used. The kinetic parameters were chosen such that the results of the simulation approximated the experimental data of our ATP concentration jumps. The parameters for ATP binding and dissociation correspond to an ATP binding constant $K_M^{ATP} = 3\ \mu M$. From the simulated curves we obtain $K_M^{ATP} = 2.5\ \mu M$ and $\tau_{2,max}^{-1} = 58\ s^{-1}$. This demonstrates that $K_{0.5}^{ATP}$ and $k_2 = \tau_{2,max}^{-1}$ are only slightly affected by the slow concentration rise at the SSM and that the parameters derived from a solution exchange experiment represent part of the kinetic properties of the enzyme.

The kinetic parameters used for the simulation are in reasonable agreement with published data. For ATP binding (see, e.g., Fendler et al., 1994) $k^+_{ATP} \approx 1 \cdot 10^7$ M^{-1} s^{-1}, $k^-_{ATP} = 94$ s^{-1}). Also, the simulations have shown not to be very sensitive to k^+_{ATP}, as long as K_M^{ATP} has the correct value.

The rate constant of Na^+ translocation is a controversial issue. In our kinetic model, k_2 represents the reaction $E_1ATP \rightharpoonup E_2P$, which is a sequence of at least two reactions $E_1ATP \rightharpoonup E_1P \rightharpoonup E_2P$. Estimations for this reaction sequence range from ~20 s^{-1} (pH 7.2, 22°C, rabbit kidney; Heyse et al., 1994) to ~200 s^{-1} (pH 7.4, 24°C, pig kidney; Kane et al., 1997; Friedrich and Nagel, 1997). In particular, most of the newer results indicate a rate constant ~200 s^{-1}.

However, the reason for the wide range of measured rates in literature is not yet clear. Aside from the fact that conditions like temperature or pH are chosen slightly differently by each author, one has to note the difference of the techniques applied. Especially in the case of fluorescence measurements (Kane et al., 1997; Steinberg and Karlish, 1989; Pratap et al., 1991) the sensing mechanism of the dyes is still under debate. Additionally, a different behavior of free membrane fragments compared to adsorbed membrane fragments cannot be excluded. In our experiments we find a relaxation rate of 60 s^{-1}, which is within the range of literature values, but somewhat lower than the 200 s^{-1} of the newer literature sources. For a more thorough discussion on the relaxation rate of Na^+ translocation, see Kane et al., 1997 or Fendler et al., 1993.

CONCLUSIONS

We present a novel method that demonstrates a rapid flow technique can be used for kinetic studies on electrical currents of the Na$^+$/K$^+$-ATPase in a reconstituted system. Under certain conditions high time resolution may be obtained, allowing the study of pre-steady-state charge translocation of ion-translocating membrane proteins. Fluid mechanical characterization of the apparatus shows the reasons for limited time resolution and yields hints for further improvement.

The system was tested with Na$^+$/K$^+$-ATPase from pig kidney. Datasets obtained by activation with ATP and Na^+ concentration jumps were in considerable agreement. The parameters determined from the measured currents are consistent with values from literature. Electrogenic Na^+ binding was demonstrated, which will be discussed in more detail in a comparison publication (Pintschovius et al., 1999). The technique is also promising for a number of different ion-translocating membrane proteins. Preliminary results have been obtained not only with Na$^+$/K$^+$-ATPase from different tissue (shark rectal gland), but also with the mitochondrial ATP-ADP-exchanger, the Na$^+$/Ca^{2+}-exchanger from lobster muscle, the electrogenic Na$^+$/H$^+$-exchanger from *Escherichia coli*, and the SR-Ca^{2+}-ATPase.

APPENDIX

Fluid dispersion between valve and cuvette

For laminar flow with a rate $\dot{V}$ through a cylinder of radius R, the Hagen-Poiseuille law describes the radial velocity distribution $u(r)$:

$$u(r) = \frac{2\dot{V}}{\pi R^2}\left(1 - \frac{r^2}{R^2}\right) \tag{13}$$

Asking for the radial location r of a streamline with velocity u, the inverse function has to be calculated:

$$r(u) = R\sqrt{1 - \frac{\pi R^2 u}{2\dot{V}}} \tag{14}$$

For the following calculation, we assume that at the location of the valve, the concentration jump from zero to c_0 be infinitely fast. Thus, at time t after the switching of the valve, the concentration at a distance x from the valve is c_0 inside an area with radius r_c, and zero outside. Writing $u = x/t$, one obtains

$$r_c = R\sqrt{1 - \frac{\pi R^2 x}{2\dot{V}t}} \tag{15}$$

At distance x the fraction of the volume already containing the "new" solution is r_c^2/R^2. The mean concentration is

$$\bar{c}(x, t) = c_0 \frac{r_c^2}{R^2} = c_0\left(1 - \frac{\pi R^2 x}{2\dot{V}t}\right) \tag{16}$$

$$c(t) = c_0\left(1 - \frac{t_0}{t}\right) \tag{17}$$

This equation holds for

$$t > t_0 = \frac{\pi R^2 x}{2\dot{V}} = \frac{V}{2\dot{V}}, \tag{18}$$

where $V = \pi R^2 x$ is the dead volume in the cylinder between the valve and a plane perpendicular to the cylinder axis at position x. For $t < t_0$, the activating solution has not yet arrived at x, so the concentration is zero. In this model, t_0 can be simultaneously interpreted as the transfer time for arrival in the cuvette and the rise time of the concentration. Assuming typical values of the experiment ($\dot{V} = 28$ ml/min, $V = 47 \pm 10$ μl) one obtains

$$t_0 = 51 \pm 11 \text{ ms}. \tag{19}$$

Numerical simulation

It was concluded that the risetime of the substrate concentration at the SSM surface is ~90 ms. In order to establish how the shape of the time-dependent signals is influenced by the slow concentration rise, we have carried out a numerical simulation using a differential equation referring to a simple kinetic problem and a time-dependent concentration $c(t)$: it was assumed that ATP-binding occurs with a second-order rate $k^+_{ATP} = 30 \cdot 10^6$ M^{-1} s^{-1} and a backward (first-order) rate $k^-_{ATP} = 90$ s^{-1} (Läuger, 1991), yielding a dissociation constant of $K = k^-_{ATP}/k^+_{ATP} = 3$ μM. In a second step electrogenic charge translocation with a rate k_2 takes place. Different values for k_2 were chosen in order to estimate how the rate $\tau^{-1}_{2,max}$ exhibited

by the simulated signal deviates from k_2.

$$ATP + E_1 \underset{k_{ATP}^-}{\overset{k_{ATP}^+}{\rightleftharpoons}} E_1ATP \overset{k_2}{\rightharpoonup} E_2P \tag{20}$$

If the states E_1 and E_1ATP are occupied N_1 and N_2-fold, the corresponding kinetic differential equation reads

$$\begin{aligned} \dot{N}_1 &= -k_{ATP}^+ c(t) N_1 + k_{ATP}^- N_2 \\ \dot{N}_2 &= k_{ATP}^+ c(t) N_1 - (k_{ATP}^- + k_2) N_2 \end{aligned} \tag{21}$$

$$N_1(0) = N_0 \tag{22}$$

$$N_2(0) = 0 \tag{23}$$

The pump current is

$$I_p(t) = k_2 \cdot N_2(t) \tag{24}$$

To enable discharge of the membrane capacitance, an electrical network (Borlinghaus et al., 1987) with a system time constant of $\tau_{sys} = 130$ ms was taken into account using the integral transformation

$$I(t) = I_0 \left[I_p(t) - \frac{1}{\tau_{sys}} \exp(-t/\tau_{sys}) \int_0^t I_p(t') \exp(t'/\tau_{sys}) dt' \right] \tag{25}$$

As the exact fluid mechanical behavior of the system is unknown, we utilized Eq. 17 derived for fluid dispersion and assumed $t_0 = \tau_{app} = 90$ ms for the concentration risetime.

Based on these assumptions the set of differential equations was solved numerically using the computer program MicroMath Scientist (Salt Lake City, UT). The results of this simulation are shown in Figs. 14 and 15.

The authors thank A. Schacht for the preparation of the Na^+/K^+-ATPase samples, K. Seifert for competent support during the preliminary experiments, and E. Bamberg for fruitful discussions and critical reading of the manuscript.

REFERENCES

Bamberg, E., H.-J. Apell, N. A. Dencher, W. Sperling, H. Stieve, and P. Läuger. 1979. Photocurrents generated by bacteriorhodopsin on planar bilayer membranes. *Biophys. Struct. Mech.* 5:277–292.

Bamberg, E., H.-J. Butt, A. Eisenrauch, and K. Fendler. 1993. Charge transport of ion pumps on lipid bilayer membranes. *Q. Rev. Biophys.* 26:1–25.

Barry, P. H., and J. M. Diamond. 1984. Effects of unstirred layers on membrane phenomena. *Physiol. Rev.* 64:763–872.

Bensimon, D., L. Kadanoff, S. Liang, B. I. Shraiman, and C. Tang. 1986. Viscous flows in two dimensions. *Rev. Mod. Phys.* 58:977–999.

Bevington, P. R. 1969. Data reduction and error analysis for the physical sciences. McGraw-Hill, New York.

Borlinghaus, R., H.-J. Apell, and P. Läuger. 1987. Fast charge translocations associated with partial reactions of the Na,K-pump. I. Current and voltage transients after photochemical release of ATP. *J. Membr. Biol.* 97:161–178.

Fendler, K., E. Grell, and E. Bamberg. 1987. Kinetics of pump currents generated by the Na^+,K^+-ATPase. *FEBS Lett.* 1:83–88.

Fendler, K., E. Grell, M. Haubs, and E. Bamberg. 1985. Pump currents generated by the purified Na^+/K^+-ATPase from kidney on black lipid membranes. *EMBO J.* 4:3079–3085.

Fendler, K., S. Jaruschewski, J. P. Froehlich, and E. Bamberg. 1994. Electrogenic and electroneutral partial reactions in Na^+/K^+-ATPase from eel electric organ. *In*, The Sodium Pump: Structure, Mechanism, Hormonal Control, and its Role in Disease. E. Bamberg and W. Schoner, editors. Springer, New York.

Fendler, K., S. Jaruschewski, A. Hobbs, W. Albers, and J. P. Froehlich. 1993. Pre-steady-state charge translocation in NaK-ATPase from eel electric organ. *J. Gen. Physiol.* 102:631–666.

Franke, C., H. Hatt, and J. Dudel. 1987. Liquid filament switch for ultra-fast exchanges of solutions at excised patches of synaptic membrane of crayfish muscle. *Neurosci. Lett.* 77:199–204.

Friedrich, T., E. Bamberg, and G. Nagel. 1996. Na^+,K^+-ATPase pump currents in giant excised patches activated by an ATP concentration jump. *Biophys. J.* 71:2486–2500.

Friedrich, T., and G. Nagel. 1997. Comparison of Na^+,K^+-ATPase pump currents activated by ATP concentration or voltage jumps. *Biophys. J.* 73:186–194.

Gadsby, D. C., and M. Nakao. 1989. Steady-state current-voltage relationship of the Na/K-pump in guinea pig ventricular myocytes. *J. Gen. Physiol.* 94:511–537.

Goldshleger, R., S. J. D. Karlish, A. Rephaeli, and W. D. Stein. 1987. The effect of membrane potential on the mammalian sodium-potassium pump reconstituted into phospholipid vesicles. *J. Physiol.* 387:331–355.

Heyse, S., I. Wuddel, H.-J. Apell, and W. Stürmer. 1994. Partial reactions of the Na,K-ATPase: determination of rate constants. *J. Gen. Physiol.* 104:197–240.

Jørgensen, P. L. 1974. Purification and characterization of (Na^+ + K^+)-ATPase. III. Purification from the outer medulla of mammalian kidney after selective removal of membrane components by sodium dodecylsulphate. *Biochim. Biophys. Acta.* 356:36–52.

Kane, D. J., K. Fendler, E. Grell, E. Bamberg, K. Taniguchi, J. P. Froehlich, and R. J. Clarke. 1997. Stopped-flow kinetic investigations of conformational changes of pig kidney Na^+,K^+-ATPase. *Biochemistry.* 36:13406–13420.

Kaplan, J. H., B. Forbush III, and J. F. Hoffman. 1978. Rapid photolytic release of adenosine 5′-triphosphate from a protected analogue: utilization by the Na:K pump of human red blood cell ghosts. *Biochemistry.* 17:1929–1935.

Läuger, P. 1991. Electrogenic Ion Pumps. Sinauer Associates, Sunderland, MA.

McCray, J. A., L. Herbette, T. Kihara, and D. R. Trentham. 1980. A new approach to time-resolved studies on ATP-requiring biological systems: laser flash photolysis of caged ATP. *Proc. Natl. Acad. Sci. USA.* 77: 7237–7241.

Nagel, G., K. Fendler, E. Grell, and E. Bamberg. 1987. Na^+ currents generated by the purified (Na^+ + K^+)-ATPase on planar lipid membranes. *Biochim. Biophys. Acta.* 901:239–249.

Pintschovius, J., K. Fendler, and E. Bamberg. 1999. Charge translocation by the Na^+/K^+-ATPase investigated on solid supported membranes: cytoplasmic cation binding and release. *Biophys. J.* 76:000–000.

Pratap, P. R., J. D. Robinson, and M. I. Steinberg. 1991. *Biochim. Biophys. Acta.* 1285:288–298.

Schwarz, W., and L. Vasilets. 1991. Variations in voltage-dependent stimulation of the Na^+/K^+ pump in *Xenopus* oocytes by external potassium. *In* The Sodium Pump: Structure, Mechanism, and Regulation. The Rockefeller University Press, New York.

Seifert, K., K. Fendler, and E. Bamberg. 1993. Charge transport by ion translocating membrane proteins on solid supported membranes. *Biophys. J.* 64:384–391.

Steinberg, M., and S. J. D. Karlish. 1989. Studies on conformational changes in Na,K-ATPase labeled with 5-iodoacetamidofluorescein. *J. Biol. Chem.* 264:2726–2734.

Xu, J., and H.-L. Li. 1995. The chemistry of self-assembled long-chain alkanethiol monolayers on gold. *J. Colloid Interface Sci.* 176:138–149.